Available online at www.sciencedirect.com

ScienceDirect

Procedia Structural Integrity 44 (2023) 386–393

Structural Integrity Procedia

www.elsevier.com/locate/procedia

XIX ANIDIS Conference, Seismic Engineering in Italy

Design tool for gypsum-sheathed cold formed steel panels under seismic action

Davide Ferrigato[a], Fabio Minghini[a,]*, Antonella Salomone[b], Nerio Tullini[a]

[a]*University of Ferrara, Dept. of Engineering DE, Via Giuseppe Saragat 1, 44122 Ferrara, Italy*
[b]*FIBRAN SpA, Via Domenico Fiasella 5/11, 16121 Genova, Italy*

Abstract

Limiting damages to nonstructural elements represents a relevant challenge for earthquake engineering. This explains why the interest for lightweight, low-damage solutions for both internal partitions and cladding is continuously increasing. In this context, wall panels made of gypsum-sheathed cold formed steel studs have become very popular in recent years, because of their ease of adaptability to various categories of building use. However, the response of these panels to both static and seismic loads still presents not completely clear features. In particular, the elastic buckling of studs under distributed vertical loads and role of sheathing-stud connections deserve to be investigated. In order to provide engineers with a comprehensive design procedure, a new calculation tool has been developed. The effects due to horizontal imposed loads and wind pressure, as well as to floor spectral acceleration are considered. All possible failure mechanisms, including stud local and distortional buckling, compression and bearing failure of gypsum sheathing, and flexural-torsional failure of top and bottom steel channels are accounted for. Stiffness and strength of the sheathing-stud and (top or bottom) channel-stud connection systems were derived from experimental tests. Some case studies are used to show the software capabilities.

Keywords: Gypsum board; Plasterboard; Cold formed steel; Nonstructural element; Out-of-plane bending; Distortional buckling.

* Corresponding author. Tel.: +39 (0)532 974912; fax: +39 (0)532 974870.
E-mail address: fabio.minghini@unife.it

2452-3216
10.1016/j.prostr.2023.01.051

1. Introduction

Damage to nonstructural components may cause partial or complete interruption of buildings' use (Baggio et al. 2007, Miyamoto 2008, Minghini et al. 2016) and determine significant economic and social losses. Hence, technological solutions providing an increased level of seismic protection are raising the interest of the scientific community. In this context, partitions comprised of gypsum-sheathed cold formed steel studs have established themselves as a winning solution due to their versatility, ease of assembly and capability to accommodate significant seismic interstorey drift demands prior to collapse (Petrone et al. 2015).

For a long period, these partitions have been designed ignoring the contribution due to gypsum boards, resulting in over-designed studs and, more in general, uneconomical configurations. Conversely, in recent years, the stiffening effect of sheathing has been highlighted (Selvaraj and Madhavan 2019). In particular, the capability of sheathing to enforce the studs to buckle in their major-axis plane, so increasing the overall partition resistance compared with the unsheathed stud case, was experimentally observed. Moreover, both experimental and analytical investigations (Lee 2000, Martin 2014, Stergiopoulos 2018) were focused on the partial composite action occurring due to connections between studs and boards. This effect is fundamental to limit the partition deflections under out-of-plane loading and must be accounted for in design.

This paper presents some findings which have allowed developing a software for the design of drywall partitions and cladding with steel studs sheathed with (generally, but not only) gypsum-based panels. Fig. 1 shows a typical internal partition with inner steel frame and two-layer sheathing on both sides. The frame is usually comprised of two horizontal C-shaped track profiles, placed one at the bottom (floor) and the other at the top (ceiling), and of vertical lipped C-shaped studs inserted into the tracks flanges and oriented so as their major axis is contained in the partition plane. A connection system made of screws of various lengths is used to join the sheathing to the frame. In fact, not only the inner sheathing layers, but also the outer ones always are connected with studs and tracks.

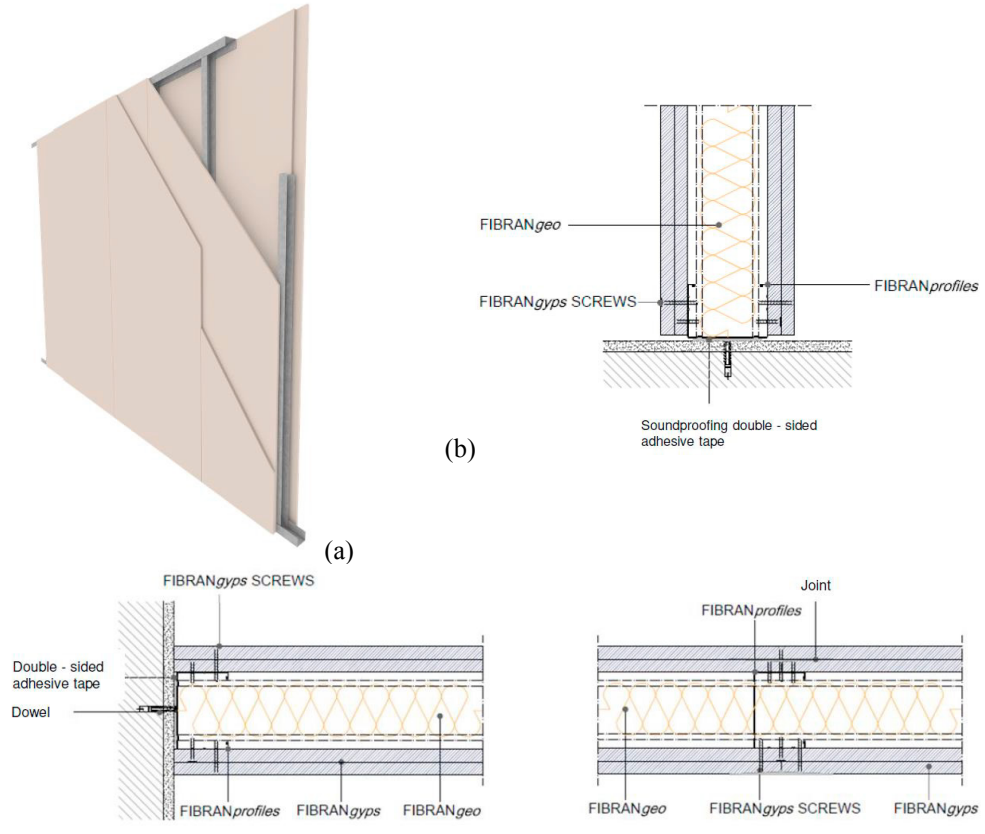

Fig. 1. Typical internal partition: (a) perspective view; (b) floor connection; (c) side wall connection and (d) stud-panel connection.

Specifically suited push-out tests were carried out to obtain measures of the stud-panel interface stiffness, and a proper model of composite beam with partial shear interaction was implemented for the calculation of out-of-plane deflections. Moreover, with regard to the stability check of steel studs in combined axial compression and major-axis bending, a refined method considering the compressive load as uniformly distributed along the stud height was proposed. For the evaluation of wind and seismic action, the pressure coefficients given by BRE (1989) and CNR (2010) and the complete formulation of floor response spectrum provided by the Italian Design Code (IMIT 2018) were implemented, respectively.

2. Experimental tests on wall subsystems

To take account of connections' contribution in limiting out-of-plane deflections of partitions, the model presented in Annex B of Eurocode 5 (CEN 2004) was implemented in the software. This model is based on Newmark's formulation for composite beam with partial shear interaction (see Tullini and Minghini 2013 and references cited herein) and involves consideration of the slip modulus of stud-sheathing connections.

Currently, there is a lack of standard regulations concerning the test setup to be used to obtain the slip modulus of stud-sheathing connections. A test setup was then designed based on the experiments by Stergiopoulos (2018), in which a symmetrical three-point test configuration was used. In particular, two studs were back-to-back connected one to another, and gypsum-based boards were jointed to stud flanges. Differentely from Stergiopoulos, who tested specimens with single-layer panels only, both single- and double-layer panels were analyzed. Type and mutual distances of screws were the same as typically used in real situations.

The experimental load-displacement plots obtained for one of the single- and one of the double-layer specimens are reported in Fig. 2(a), whereas Fig. 2(b) shows a typical failure mode. It can be noted that for the double-layer case, both elastic stiffness and peak strength are doubled compared with the single-layer case. This justifies the adoption of a slip modulus depending on the specific wall configuration to be considered.

The composite beam model also needs the elastic modulus of sheathing and should provide the stress state in the boards for strength calculations. The software neglects the contribution due to plasterboard in tension, but allows for local checks of compressive strength of panels. Therefore, a number of preliminary compression tests were carried out to estimate elastic modulus the compressive strength of boards (Fig. 3(a)). Both standard- and high-density boards were tested, with the latter showing higher strength and stiffness than the former. Presently, the collected data are not

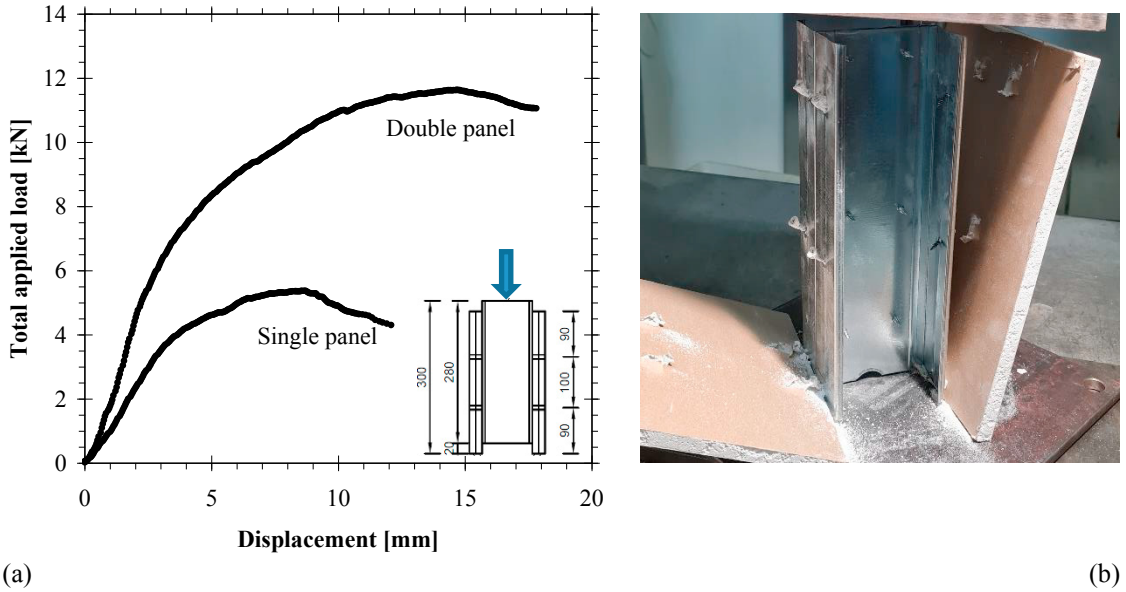

Fig. 2. Push-out test: (a) experimental load-displacement plot for sheathing with one (single panel) and two layers per side (double panel); (b) single panel case, specimen at the end of test.

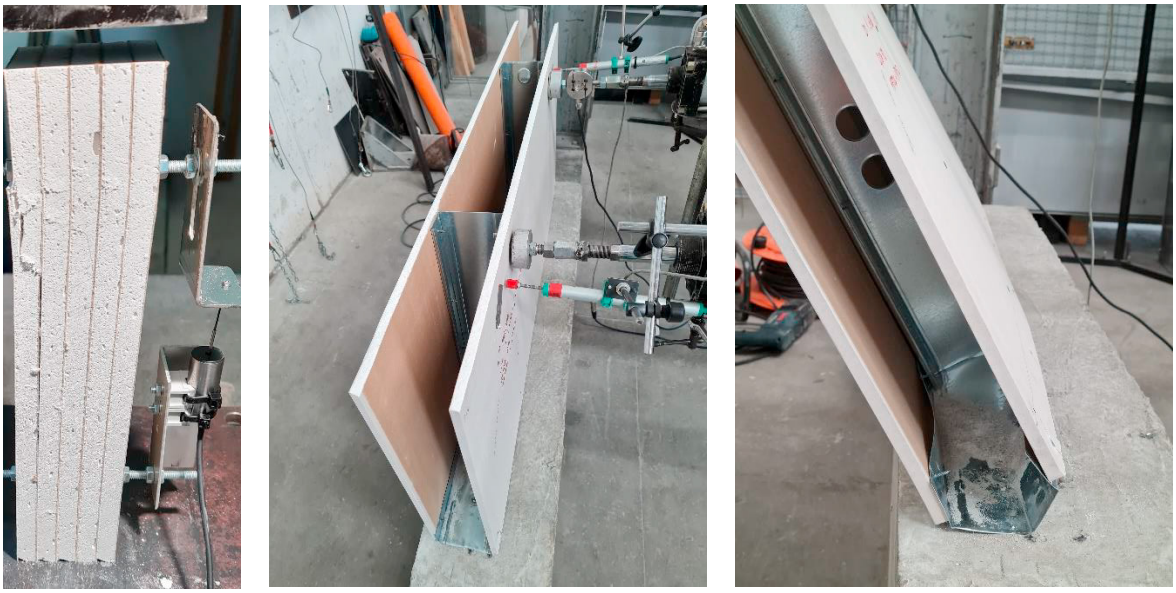

(a) (b) (c)

Fig. 3. (a) Compression test on gypsum specimen comprised of five 12.5-mm thick layers; out-of-plane bending test on the bottom connection of a gypsum-sheathed partition: (b) specimen at the beginning of test and (c) failure of the track profile.

still enough for a statistical analysis of mechanical properties such as that presented by Petrone et al. (2016). On the safe-side values are then imposed in the software.

Finally, in order to establish a mechanical model suitable for strength verification of wall-floor connection, out-of-plane bending tests on subsytems (Fig. 3(b)) comprised of bottom track profile, two pieces of studs and portions of plasterboard on both sides were performed. To reproduce the actual joint at floor level, the track profile was connected with a concrete block. The tests highlighted a very high rotational capacity of the joint and a fundamental contribution of boards in limiting excessive deformations of track flanges (Fig. 3(c)).

3. ULS design of studs under bending and axial compression

Out-of-plane bending of partitions, involving bending of studs in their major-axis plane, may be due to horizontal imposed loads according with the relevant category of use, wind, earthquake or a combination of these actions. In the context of an “all steel design” approach, i.e., ignoring the contribution of sheathing, the corresponding failure modes will involve local-distortional, as well as flexural- or lateral-torsional buckling of studs. However, as was shown by Selvaraj and Madhavan (2018, 2019), for typical internal partitions comprised of studs with sheathing on both sides, the stiffening effect of gypsum sheets and their connections with stud flanges may be able to restrain lateral-torsional buckling of studs. This effect seems particularly important for high values of stud global slenderness and, as expected, is influenced by type and spacing of sheathing-stud connectors. Analogous results were obtained, for similar technologies, by other researchers (see for example the paper by Fiorino et al. 2018).

In this paper, lateral-torsional buckling of studs is then ignored. Hence, in the presence of axial compression due to self weight combined with out-of-plane bending, each stud must satisfy the following expression valid for class 4 sections:

$$\frac{\gamma_{M1} N_{Ed}}{\chi_y N_{Rk}} + k_{yy} \frac{\gamma_{M1}\left(M_{y,Ed} + \Delta M_{y,Ed}\right)}{M_{y,Rk}} \le 1\,, \tag{1}$$

which was derived from Eq. 6.2 reported by CEN (2005) with $\chi_{LT} = 1$ (see also the ECCS document by Dubina et al. 2012). Equation (1) assumes that stud buckling takes place in the major-axis (*xy*) plane and relies upon the on the safe-side assumption that no restraint to stud buckling is provided by gypsum sheets. Coefficient χ_y represents the usual reduction factor for flexural buckling, k_{yy} is an interaction factor depending on elastic critical load and bending moment diagram, whereas $\gamma_{M1} = 1.05$ (IMIT 2018) is the partial safety factor to be used for stability assessment. Moreover, moment $\Delta M_{y,Ed}$ depends on the shift of the centroidal axis for class 4 sections subjected to pure compression (CEN 2006b). Due to symmetry of stud cross-section with respect to the major axis, $\Delta M_{y,Ed} = 0$. Terms N_{Ed} and $M_{y,Ed}$ indicate the design values of the compressive load and maximum moment about the *y*-axis, respectively.

Substituting effective cross-sectional properties $A_{eff} = N_{Rk}/f_{yk}$ and $W_{eff,y} = M_{y,Rk}/f_{yk}$ into Eq. (1), and adopting the calculation method outlined in Annex A of CEN (2005), the previous condition can be rewritten as follows:

$$\frac{\gamma_{M1} N_{Ed}}{\chi_y A_{eff} f_{yk}} + \frac{C_{my} C_{mLT} \gamma_{M1} M_{y,Ed}}{\left(1 - \chi_y \frac{N_{Ed}}{N_{cr,y}}\right) W_{eff,y} f_{yk}} \leq 1, \tag{2}$$

where $N_{cr,y}$ is the critical load of instability in the major-axis plane. In the absence of torsional deformations, $C_{mLT} = 1$ and $C_{my} = C_{my,0}$, with $C_{my,0}$ being related with bending moment diagram. In particular, for linearly varying moment and $\psi = 0$ in Table A.2 of CEN (2005), $C_{my,0} = 0.79–0.12 N_{Ed}/N_{cr,y}$; finally, for concentrated load at midheight and uniformly distributed load with pinned ends, $C_{my,0} = 1–0.18 N_{Ed}/N_{cr,y}$ and $1+0.03 N_{Ed}/N_{cr,y}$, respectively. Therefore, in the case of horizontal imposed load, an on the safe-side prediction may be obtained assuming $C_{my,0} = 1$. Equation (2) may the be rewritten as:

imposed load (concentrated):
$$\frac{\gamma_{M1} N_{Ed}}{\chi_y A_{eff} f_{yk}} + \frac{1}{1 - \chi_y \frac{N_{Ed}}{N_{cr,y}}} \frac{\gamma_{M1} M_{y,Ed}}{W_{eff,y} f_{yk}} \leq 1 \tag{3}$$

wind and earthquake load (uniformly distributed):
$$\frac{\gamma_{M1} N_{Ed}}{\chi_y A_{eff} f_{yk}} + \frac{1 + 0.03 \frac{N_{Ed}}{N_{cr,y}}}{1 - \chi_y \frac{N_{Ed}}{N_{cr,y}}} \frac{\gamma_{M1} M_{y,Ed}}{W_{eff,y} f_{yk}} \leq 1 \tag{4}$$

An alternative approach is reported by CEN (2006a) and based on the following interaction formula (see also Dubina et al. 2012):

$$\left(\frac{N_{Ed}}{N_{b,Rd}}\right)^{0.8} + \left(\frac{M^{II}_{y,Ed}}{M_{b,Rd}}\right)^{0.8} \leq 1, \tag{5}$$

where $N_{b,Rd} = \chi_y A_{eff} f_{yk}/\gamma_{M1}$ should be viewed as the design resistance of the stud for flexural buckling in the major-axis plane, $M_{b,Rd} = \chi_{LT} W_{eff,y} f_{yk}/\gamma_{M1}$ is given the meaning of design resistance for lateral-torsional buckling which, for torsionally restrained stud ($\chi_{LT} = 1$), coincides with the design moment for flexural failure in the major-axis plane and, finally, $M^{II}_{y,Ed}$ is the second order moment including possible effects due to centroid shift (which are not relevant for the studs as was mentioned before).

In the software development, it was decided to perform the studs check for buckling under combined compression and major-axis bending with both approaches, i.e., the stud should satisfy the most unfavourable condition between

Eq. (3) (or (4), depending on the moment diagram) and Eq. (5). Due to the shape of stud cross-section, reduction coefficient χ_y was always calculated based on buckling curve b in accordance with CEN (2006a).

3.1. Stud buckling under distributed compressive load

As an improvement in the method usually adopted to check stability, which assumes the self weight of sheathing as being concentrated at the stud top end, a more realistic loading model with the stud subjected to a uniformly distributed axial load g was considered, leading to a compressive stress resultant variable along the height. Assuming pinned ends, this load condition would yield the following buckling load (Elishakoff 2005):

$$(gH)_{cr} = 18.6\,EI/H^2\,, \tag{6}$$

where H indicates the stud height and EI is the bending rigidity relative to the buckling plane. Compared with the case of compressive loads concentrated at the ends, $(gH)_{cr}$ results $18.6/\pi^2 = 1.88$ times greater. Correspondingly, other conditions being equal, the nondimensional slenderness (defined by CEN 2005, Sect. 6.3.1.2) turns out to be $1.88^{0.5} = 1.37$ times smaller, so influencing beam-column ultimate resistance.

Finite Element (FE) beam models of two steel studs with $H = 3$ and 5 m were developed in STRAND7® (2004). Geometrically nonlinear analyses of the studs subjected to a uniformly distributed, incremental axial load were carried out in the presence of an imperfection in the form of concentrated force of 100 N at midheight producing bending in the major-axis plane. The plots of nondimensional axial load $gH/(gH)_{cr}$ vs. ratio u/u^{I} between total and first-order horizontal displacements at midheight are reported in Fig. 4(a), whereas Fig. 4(b) shows the numerical results in terms of $gH/(gH)_{cr}$ vs. ratio $M_{y,Ed}/M_{y,Ed}^{I}$ between maximum total and first-order bending moment in the major-axis plane (symbols). Also reported in Fig. 4(b) are functions of the form $1/[1-gH/(gH)_{cr}]$ (solid lines), which provide a good approximation to the numerical solutions. In particular, for the studs with $H = 3$ and 5 m, this approximation is on the safe side for $gH/(gH)_{cr} \le 0.73$ and $gH/(gH)_{cr} \le 0.88$, respectively. This justifies the use of term $1/[1-gH/(gH)_{cr}]$ as amplification factor for the first-order moment.

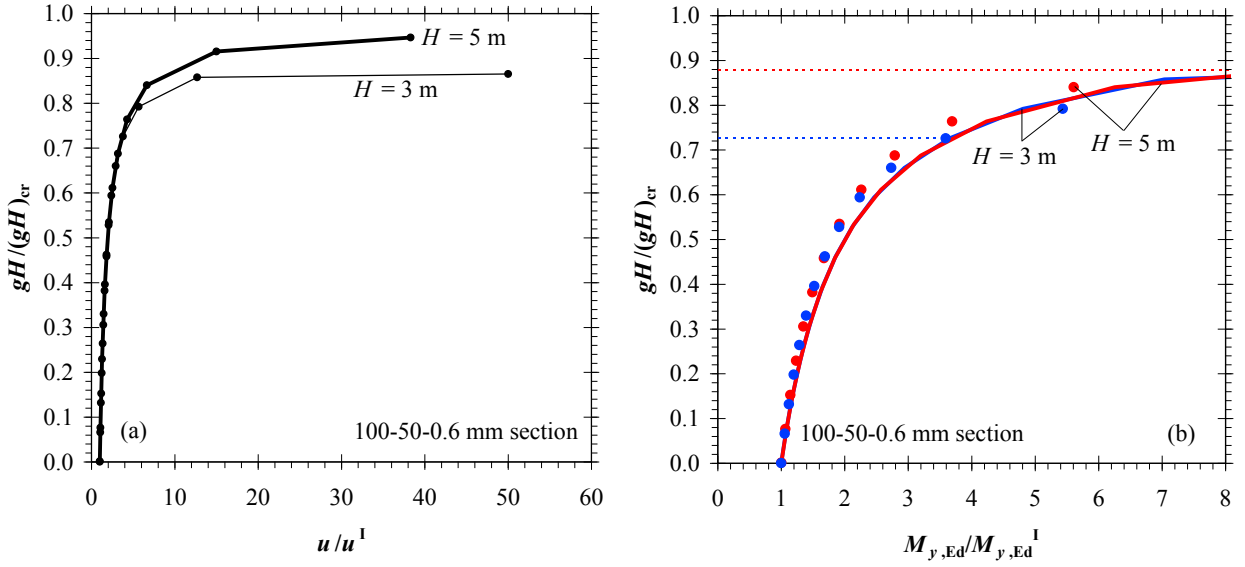

Fig. 4. Geometrically nonlinear analysis of steel studs with cross-section dimensions 100-50-0.6 mm and height of 3 and 5 m: nondimensional plots of axial load vs. (a) lateral displacement and (b) bending moment at midheight. In (b), FE analysis results (symbols) are compared with amplification factor $1/[1-gH/(gH)_{cr}]$ (solid lines).

Table 1. Comparison between distributed and concentrated compressive load assumptions: nondimensional lenderness (λ_y), reduction factor (χ_y), axial load ratio ($N_{Ed}/N_{cr,y}$), moment ratio [$M_{y,Ed}/(W_{eff,y}f_{yk})$] and calculated Left-Hand Sides (LHS) of Eqs. (4) and (5).

Type of axial load	λ_y	χ_y	$N_{Ed}/N_{cr,y}$	$M_{y,Ed}/(W_{eff,y}f_{yk})$	Eq. (4), LHS	Eq. (5), LHS
Distributed	1.00	0.60	0.30	0.20	0.79	0.98
Concentrated	1.37	0.39	0.57	0.20	1.08	1.40

A simple numerical example is presented in Table 1 to show the improvement in stud design obtained by using the distributed, rather than the concentrated, axial load assumption. In particular, a stud under distributed axial compression having nondimensional slenderness for flexural buckling into the major-axis plane $\lambda_y = 1$ was considered. The maximum axial load at the bottom end was assumed to be 30% of the buckling load provided by Eq. (6). Moreover, a uniformly distributed horizontal load was assumed, yielding a maximum first-order bending moment about the major-axis equal to 20% of bending resistance $W_{eff,y} f_{yk}$. The calculations indicate that both of the requirements (4) and (5) are fulfilled. Conversely, if the maximum axial compression of the previous case is supposed concentrated at the top end section, the stud results to be unsafe.

4. Conclusions

This paper reports some experimental and analytical findings which have allowed developing a software tool for the design of drywall partitions with steel cold formed thin-walled profiles and gypsum-based sheathing.

The tests on the floor joint confirmed the fundamental contribution of sheathing and highlighed a significant out-of-plane rotational capacity of the system.

From the push-out tests, suitable values of the slip modulus were obtained for use in a composite beam model with partial shear interaction. This model provides a more realistic representation of the actual partition behaviour at the serviceability limit state, and may be rearranged for strength checks at the ultimate limit state.

The criterion usually adopted to check stud stability in the major-axis plane was reviewed to take account of the actual distribution of compressive stresses along the stud height. This proposal helps limiting the stud cross-section dimensions and avoiding unnecessary and costly overdesigns.

Both in- and out-of-plane tests on full scale partitions will allow to further improve the knowledge of the actual system and adjust the design tool.

Acknowledgements

This research was supported by FIBRAN SpA. The experimental tests were designed at the University of Ferrara and carried out by Istituto Giordano SpA at the Security & Safety Lab in Gatteo (FC), Italy.

References

Baggio, C., Bernardini, A., Colozza, R., et al., 2007. Field Survey for Post-Earthquake Damage and Safety Assessment and Short Term Countermeasures (AeDES) (Pinto, A.V., and Taucer, F., Eds.), EUR 22868 EN, ISSN 1018-5593, Joint Research Centre, Institute for the Protection and Security of Citizen.

BRE (Building Research Establishment), 1989. The assessment of wind loads, Digest 346, ISBN 0 85125 473 X, Garston, Watford.

CEN (European Committee for Standardization), 2005. Eurocode 3. Design of steel structures – Part 1-1: General rules and rules for buildings, EN 1993-1-1:2005, Brussels, 2005.

CEN (European Committee for Standardization), 2006a. Eurocode 3. Design of steel structures – Part 1-3: General rules – Supplementary rules for cold-formed members and sheeting, EN 1993-1-3:2006, Brussels, 2006.

CEN (European Committee for Standardization), 2006b. Eurocode 3. Design of steel structures – Part 1-5: Plated structurl elements, EN 1993-1-5:2006, Brussels, 2006.

CEN (European Committee for Standardization), 2004. Eurocode 5. Design of timber structures – Part 1-1: General – Common rules and rules for buildings, EN 1995-1-1:2004, Brussels, 2004.

CNR (National Research Council of Italy), 2010. Guide for the assessment of wind actions and effects on structures, CNR-DT 207/2008, Rome.

Dubina, D., Ungureanu, V., Landolfo, R., 2012. Design of cold-formed steel structure. European Convention for Constructional Steelwork, 1st Ed., 654 pp.

Elishakoff, I., 2005. Eigenvalues of inhomogeneous structures – Unusual closed-form solutions, CRC Press, Boca Raton.
Fiorino, L., Pali, T., Landolfo, R., 2018. Out-of-plane seismic design by testing of non-structural lightweight steel drywall partition walls. Thin-Walled Structures, 130, 213-230.
IMIT (Italian Ministry of Infrastructures and Transports), 2018. Norme tecniche per le costruzioni, DM 17/01/2018 [In Italian].
Lee, Y.-k., 2000. Behavior of gypsum-sheathed cold-formed steel wall stud panels. PhD Thesis, Oregon State University.
Martin, G., 2014. Investigation of the slip modulus between cold-formed steel and plywood sheathing. MSc Thesis, Kansas State University.
Minghini, F., Ongaretto, E., Ligabue, V., Savoia, M., Tullini, N., 2016. Observational failure analysis of precast buildings after the 2012 Emilia earthquakes. Earthquakes and Structures 11(2), 327-346.
Miyamoto, H.K., 2008. China Earthquake Field Investigation Report, Sichuan, China M8 Earthquake, Global Risk Miyamoto, May.
Petrone, C., Magliulo, G., Lopez, P., Manfredi G., 2015. Seismic fragility of plasterboard partitions via in-plane quasi-static tests. Earthquake Engineering and Structural Dynamics 44, 2589-2606.
Petrone, C., Magliulo, G., Manfredi G., 2016. Mechanical properties of plasterboards: experimental tests and statistical analysis. Journal of Materials in Civil Engineering 28(11), 04016129.
Selvaraj, S., Madhavan, M., 2018. Studies on cold-formed steel stud panles with gypsum sheathing subjected to out-of-plane bending. Journal of Structural Engineering, 144(9), 04018136.
Selvaraj, S., Madhavan, M., 2019. Investigation on sheathing effect and failure modes of gypsum sheathed cold-formed steel wall panels subjected to bending. Structures, 17, 87-101.
Stergiopoulos, M., 2018. Modelling of the stiffening effects of boards on cold-formed steel wall panels. PhD Thesis, University of Surrey.
STRAND7® (2004). Theoretical manual —theoretical background to the Strand7 finite element analysis system, First ed.
Tullini, N., Minghini, F., 2013. Nonlinear analysis of composite beams with concrete-encased steel truss. Journal of Constructional Steel Research 91, 1-13.